

# Oxidation of *N*-(4-Chlorophenyl)-*N'*-hydroxyguanidine to *N*-(4-Chlorophenyl)urea and Nitric Oxide by Photoexcited Iron Porphyrins

Andrea Maldotti,<sup>[a]</sup> Alessandra Molinari,<sup>[a]</sup> Irene Vitali,<sup>[a]</sup> Elena Ganzaroli,<sup>[a]</sup>  
 Pierrette Battioni,<sup>[b]</sup> Delphine Mathieu,<sup>[b]</sup> and Daniel Mansuy<sup>[b]</sup>

**Keywords:** O–O activation / Nitric oxide / Photooxidation / Porphyrins / Protein models

Photochemical excitation ( $\lambda > 350$  nm) of chloro[*meso*-tetrakis(2,6-dichlorophenyl)porphyrin]iron(III) [ $\text{Fe}^{\text{III}}(\text{TDCPP})\text{Cl}$ ] and chloro[*meso*-tetra( $\alpha, \alpha, \alpha, \alpha$ -pivalamidophenyl)porphyrin]iron(III) [ $\text{Fe}^{\text{III}}(\text{TpivPP})\text{Cl}$ ] induces the oxidation of coordinated *N*-(4-chlorophenyl)-*N'*-hydroxyguanidine (**1**) by molecular oxygen, to give iminoxyl radicals and the  $\text{Fe}^{\text{II}}(\text{O}_2)$  [or  $\text{Fe}^{\text{III}}(\text{O}_2^-)$ ] adduct. This complex can be accumulated in significant amounts using [ $\text{Fe}^{\text{III}}(\text{TpivPP})\text{Cl}$ ]. The primary photoproducts give rise to secondary reactions that lead to the formation of *N*-(4-chlorophenyl)urea (**2**) as the main end-product of **1**. The conversion of **1** into **2** is accompanied by the formation of NO, as revealed both by an ESR spin-trapping technique and in the form of its stable end-products

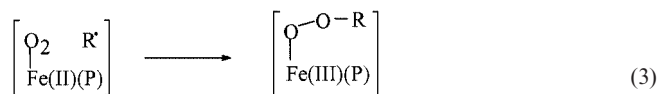
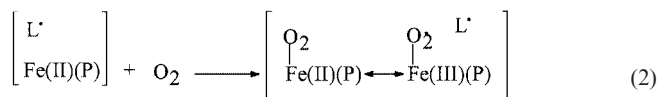
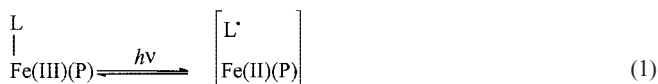
$\text{NO}_2^-$  and  $\text{NO}_3^-$ . The presence of 1-methyl imidazole (1-MeIm) coordinated in axial position has a significant positive effect on the photoinduced production of **2** and NO from the hydroxyguanidine **1**. The observation that radical scavengers inhibit the photooxidation process strongly supports the possibility that the reaction pathway resembles a radical-type autoxidation mechanism, where the very fast reaction of  $\text{O}_2$  with the ferrous porphyrin in the presence of the photo-generated iminoxyl radical should yield an iron-peroxo intermediate as precursor of the urea **2** and NO.

(© Wiley-VCH Verlag GmbH & Co. KGaA, 69451 Weinheim, Germany, 2004)

## Introduction

The photochemical excitation of iron porphyrin complexes [ $\text{Fe}^{\text{III}}(\text{P})$ ] is an important tool for obtaining biomimetic model systems of interest in oxygenase-like catalytic oxidation.<sup>[1]</sup> All these systems are characterized by common primary photoprocesses. Irradiation in axial ligand (L) to metal charge-transfer bands ( $\lambda = 300\text{--}400$  nm) induces a homolytic cleavage of the  $\text{Fe}^{\text{III}}(\text{L})$  bond, which causes oxidation and detachment of L as a radical species and reduction of  $\text{Fe}^{\text{III}}$  to  $\text{Fe}^{\text{II}}$  [Equation (1)]. It has been demonstrated that  $\text{O}_2$  is able to effectively react with the ferrous intermediate, thus inhibiting solvent-cage effects [back reaction in Equation (1)]. A peculiar aspect of this process is that a monoelectronic reductive activation of  $\text{O}_2$  occurs through the formation of a dioxyiron complex  $\text{Fe}^{\text{II}}(\text{P})(\text{O}_2)$  or  $\text{Fe}^{\text{III}}(\text{P})(\text{O}_2^-)$  according to Equation (2). A two-electron reduction of  $\text{O}_2$  may also be achieved when the described photochemical process is carried out in the presence of suitable hydrocarbons (RH). Under these conditions, alkyl radicals ( $\text{R}^\cdot$ ) may be formed as a consequence of the reaction between the photogenerated L $^\cdot$  radicals and RH. The ex-

tremely fast subsequent reaction of  $\text{O}_2$  with  $\text{Fe}^{\text{II}}(\text{P})$  in the presence of  $\text{R}^\cdot$  may lead to the formation of alkyl-peroxo complexes according to Equation (3).<sup>[2]</sup> In all cases, the photoassisted activation of  $\text{O}_2$  occurs in a catalytic manner, since the starting iron porphyrin is restored after its reoxidation and after coordination of a new equivalent of axial ligand.



<sup>[a]</sup> Dipartimento di Chimica Università di Ferrara, Sezione ISOF–CNR, Via Luigi Borsari 46, 44100 Ferrara, Italy

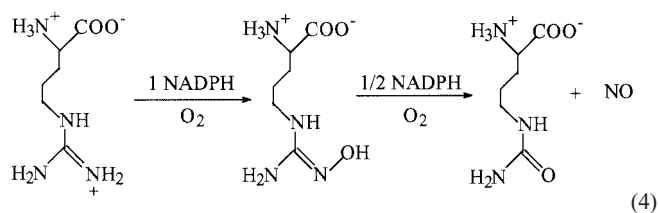
<sup>[b]</sup> Laboratoire de Chimie et Biochimie Pharmacologiques Toxicologiques, UMR 8601 CNRS, Université Paris V, 45 rue des Saints Pères, 75270 Paris Cedex 06, France

Chloro[*meso*-tetrakis(2,6-dichlorophenyl)porphyrin]iron(III) [ $\text{Fe}^{\text{III}}(\text{TDCPP})\text{Cl}$ ] has been often employed in the photocatalytic activation of  $\text{O}_2$  as the bulky chlorine atoms in its *meso*-aryl groups prevent the well-known bimolecular

reaction of the  $\text{Fe}^{\text{II}}$ dioxy complex to give  $\mu$ -oxo dimers as the final product.<sup>[3]</sup> Moreover, they provide a steric protection of the porphyrin ring against its radical-induced oxidative degradation.<sup>[4]</sup>

One intriguing and up-to-date aspect of the photocatalytic processes described above is their possibility to generate reactive intermediates such as  $\text{Fe}^{\text{III}}(\text{P})(\text{O}_2^\cdot)$ ,  $\text{Fe}^{\text{III}}(\text{P})(\text{OOR})$  and radical species that might be relevant also to the mechanism of nitric oxide synthases (NOSs), as explained below.

All the three NOS isoforms in mammals catalyse the stepwise oxidation of L-arginine to nitric oxide (NO) by  $\text{O}_2$  and NADPH.<sup>[5]</sup> This process occurs in the NOS oxygenase domain, which contains heme and tetrahydrobiopterin (usually indicated as  $\text{BH}_4$ ) as cofactors.<sup>[6]</sup> The NO synthesis mechanism is complex and not completely understood. A first step is likely a classical monooxygenation of L-arginine to give *N*-hydroxy-L-arginine, which occurs with the consumption of one mol of  $\text{O}_2$  and one mol of NADPH [first step in Equation (4)]. The generally accepted P450 reaction mechanism can account for the stoichiometry and the product formation.<sup>[7]</sup> Reduction of ferric heme is followed by the formation of a  $\text{Fe}^{\text{II}}$ dioxy complex that accepts a second electron from NADPH to form an iron-peroxo intermediate. The subsequent O–O bond scission yields a presumed iron-oxo species that is able to hydroxylate a guanidinic nitrogen of L-arginine.



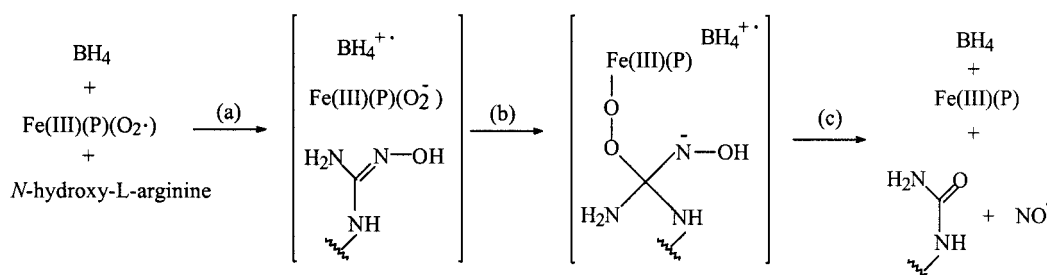
The second step involves an oxidative cleavage of the C=NOH bond of *N*-hydroxy-L-arginine to give the final products NO and L-citrulline through the consumption of one mol of  $\text{O}_2$  and only one electron coming from 0.5 mol of NADPH [second step in Equation (4)].<sup>[8]</sup> A monoelectronic reduction of ferric heme enables  $\text{O}_2$  binding and forms an iron-dioxy complex [ $\text{Fe}^{\text{II}}(\text{P})(\text{O}_2)$  or  $\text{Fe}^{\text{III}}(\text{P})(\text{O}_2^\cdot)$ ]. A number of experimental results are consistent with  $\text{BH}_4$  having a

redox function in the second step of NO synthesis. Stuehr et al.<sup>[9]</sup> have proposed that the cofactor  $\text{BH}_4$  may be able to provide a second electron to  $\text{Fe}^{\text{III}}(\text{P})(\text{O}_2^\cdot)$  to yield an iron-peroxo intermediate as ultimate oxidant able to react with bound *N*-hydroxy-L-arginine according to Scheme 1 (steps a and b). The subsequent back electron transfer to the  $\text{BH}_4^{+\cdot}$  radical should yield the final products NO and L-citrulline together with  $\text{BH}_4$  and  $\text{Fe}^{\text{III}}(\text{P})$  in their starting conditions (step c).

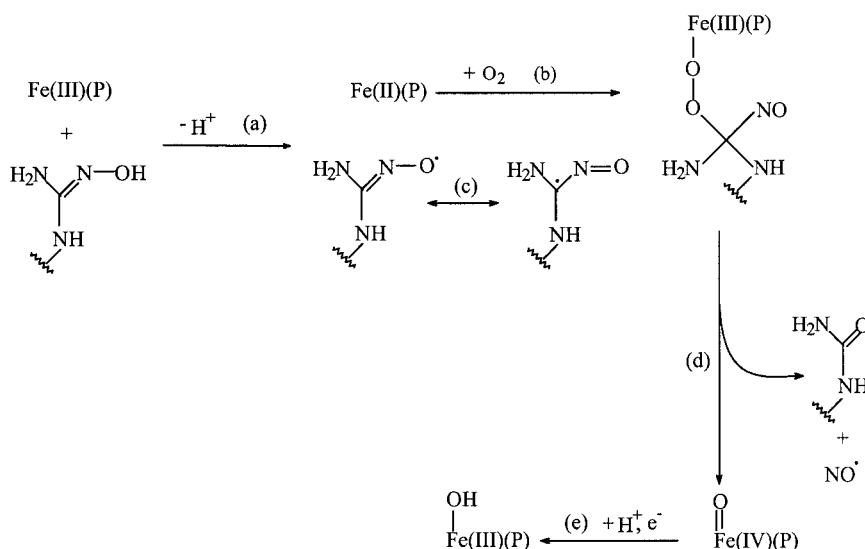
The formation of radical intermediates has been proposed by Groves et al.<sup>[5d,10]</sup> for model systems that mimic many important properties of the NOS-catalysed oxidation of *N*-hydroxy-L-arginine. This mechanism, summarized in Scheme 2, involves the oxidation of *N*-hydroxy-L-arginine to the corresponding iminoxyl radical with the simultaneous reduction of  $\text{Fe}^{\text{III}}(\text{P})$  to  $\text{Fe}^{\text{II}}(\text{P})$  (step a). The insertion of  $\text{O}_2$  between the ferrous porphyrin and the radical in its  $\alpha$ -nitroso form would generate an iron-peroxo intermediate (steps b and c). The subsequent homolytic cleavage of its O–O bond may lead to the formation of NO, L-citrulline and  $\text{Fe}^{\text{IV}}(\text{P})(\text{O})$  (step d), which can immediately undergo a single-electron reduction with, possibly, the involvement of  $\text{BH}_4$  (step e).

The very limited number of substrates for NOSs known so far suggests that highly specific structural features are required for NO generation by these enzymes. However, it has been recently shown that NOSs are also able to catalyse the oxidation of some analogues of *N*-hydroxy-L-arginine.<sup>[11]</sup> In particular, it has been found that mixtures of *N*-aryleurea, *N*-arylcyanamide and NO are formed when several *N*-aryl-*N'*-hydroxyguanidines are incubated in the presence of NOS. These substrates are of particular interest in mechanistic studies with model systems since, contrary to *N*-hydroxy-L-arginine, their oxidation products are relatively stable and easy to analyse.

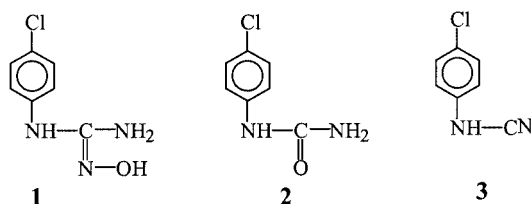
In this work, we have used as oxidizable substrate a simple *N*-aryl-*N'*-hydroxyguanidine: *N*-(4-chlorophenyl)-*N'*-hydroxyguanidine (**1**, see Scheme 3). We have investigated its redox reactivity in the presence of photoexcited iron porphyrins with the aim of inducing the reductive activation of  $\text{O}_2$  in order to obtain intermediates analogous to those involved in the NOS-dependent oxidation of *N*-hydroxy-L-arginine. The possibility that the photoinduced redox processes may be affected by the presence of *N*-methylimidazole (1-MeIm) has also been evaluated.



Scheme 1. Proposed mechanism for NOS-assisted oxidation of *N*-hydroxy-L-arginine



Scheme 2. Proposed radical-type mechanism

Scheme 3. *N*-(4-Chlorophenyl)-*N*'-hydroxyguanidine (**1**), *N*-(4-chlorophenyl)urea (**2**) and *N*-(4-chlorophenyl)cyanamide (**3**)

The iron porphyrins employed are shown in Figure 1. [Fe<sup>III</sup>(TDCPP)Cl] has been chosen because of its stability under photocatalytic conditions. The chloro[*meso*-tetra( $\alpha,\alpha,\alpha,\alpha$ -pivalamidophenyl)porphyrin]iron(III) [Fe<sup>III</sup>(TpivPP)Cl] is expected to give important information about the possible formation and reactivity of Fe<sup>II</sup>(P)(O<sub>2</sub>) adducts as it has a protective enclosure for binding oxygen on one side of the porphyrin ring and it is able to form a stable adduct with O<sub>2</sub>.<sup>[12]</sup>

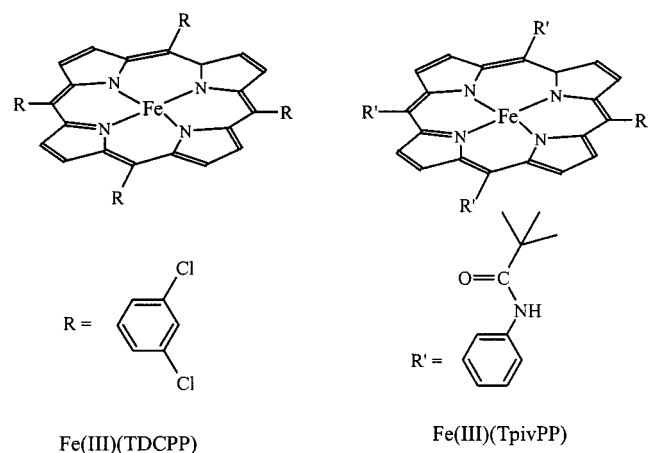


Figure 1. Structure of the investigated iron porphyrins

## Results and Discussion

### Biomimetic Photooxidation of *N*-(4-Chlorophenyl)-*N*'-hydroxyguanidine (**1**)

The photochemical experiments described below were carried out by irradiating CH<sub>3</sub>CN solutions of [Fe<sup>III</sup>(TDCPP)Cl] ( $1 \times 10^{-5}$  M) and **1** ( $1 \times 10^{-3}$  M) in the presence of 1-MeIm, ( $5 \times 10^{-5}$  M) [Fe<sup>III</sup>(TDCPP)Cl/**1**/1-MeIm system] or without 1-MeIm [Fe<sup>III</sup>(TDCPP)Cl/**1** system] with light of wavelength higher than 350 nm. First of all, we report some UV/Vis results shedding light on the nature of the main light-absorbing species present in these systems. More specifically, we were interested in defining the nature of the iron porphyrin axial ligand that may be involved in the primary photochemical process in Equation (1).

It has been reported previously that numerous *N*-hydroxyguanidines such as **1** are able to bind through their oxygen atom to the ferric heme group of both microperoxidase-8 and NOS itself.<sup>[13]</sup> The consequent formation of stable, low-spin complexes is accompanied by significant changes in the UV/Vis spectra. In particular, the coordination of *N*-hydroxyguanidines causes red shifts of the Soret peak. Table 1 (runs a and b) provides evidence that the addition of **1** to a [Fe<sup>III</sup>(TDCPP)Cl] solution induces an analogous shift of the Soret band from 412 nm to 422 nm, thus indicating that **1** is coordinated in the axial position to the metal centre to give the complex [Fe<sup>III</sup>(TDCPP)(**1**)Cl]. Table 1 (run c) and Figure 2 show that different spectral variations were obtained when both **1** and 1-MeIm were added to [Fe<sup>III</sup>(TDCPP)Cl]. This result, together with the observation that addition of 1-MeIm alone causes other spectral changes (run d) allows us to infer that solution equilibria in the [Fe<sup>III</sup>(TDCPP)Cl]/**1**/1-MeIm system lead mainly to the formation of a porphyrin complex that contains hydroxyguanidine and 1-MeIm bound in the two axial positions (step a in Scheme 4).

Table 1. UV/Vis spectroscopic data of  $[\text{Fe}^{\text{III}}(\text{TDCPP})\text{Cl}]$ 

Run	System <sup>[a]</sup>	Absorption maxima (nm)
a	$\text{Fe}^{\text{III}}(\text{TDCPP})\text{Cl}$	325, 412, 570
b	$\text{Fe}^{\text{III}}(\text{TDCPP})\text{Cl}/\mathbf{1}$	422, 541
c	$\text{Fe}^{\text{III}}(\text{TDCPP})\text{Cl}/\mathbf{1}/\mathbf{1}\text{-MeIm}$	426, 535
d	$\text{Fe}^{\text{III}}(\text{TDCPP})\text{Cl}/\mathbf{1}\text{-MeIm}$	327, 413, 569
e	$\text{Fe}^{\text{III}}(\text{TDCPP})\text{Cl}/\mathbf{1}/\mathbf{1}\text{-MeIm}/h\nu$	416, 505, 546

[a]  $[\text{Fe}^{\text{III}}(\text{TDCPP})\text{Cl}]$  ( $\text{CH}_3\text{CN}$ ):  $1 \times 10^{-5}$  M;  $[\mathbf{1}]$ :  $1 \times 10^{-3}$  M;  $[\mathbf{1}\text{-MeIm}]$ :  $5 \times 10^{-5}$  M. Irradiation in run e was carried out at  $22 \pm 1$  °C in the presence of 760 Torr of oxygen; excitation wavelength:  $\lambda > 350$  nm; irradiation time: 30 min.

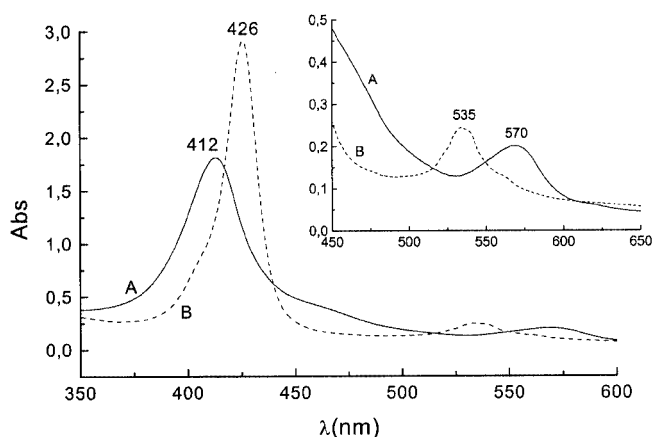


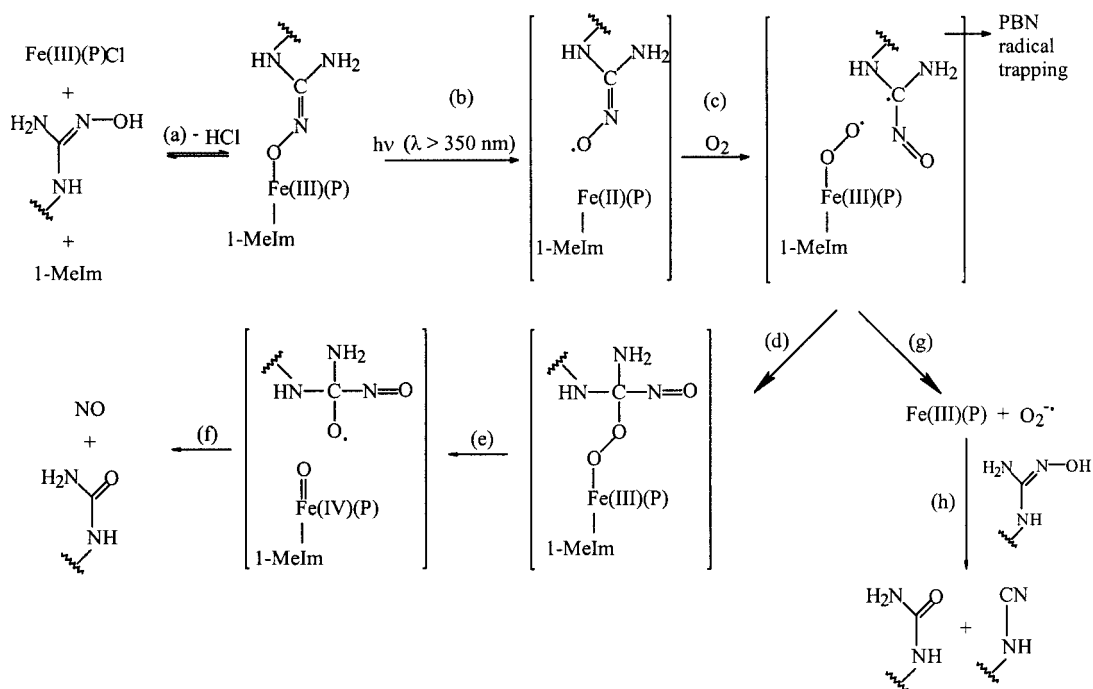
Figure 2. A) UV/Vis spectrum of a  $\text{CH}_3\text{CN}$  solution of  $[\text{Fe}^{\text{III}}(\text{TDCPP})\text{Cl}]$  ( $1 \times 10^{-5}$  M); B) UV/Vis spectrum of a  $\text{CH}_3\text{CN}$  solution of  $[\text{Fe}^{\text{III}}(\text{TDCPP})\text{Cl}]$  ( $1 \times 10^{-5}$  M) in the presence of  $\mathbf{1}$  ( $1 \times 10^{-3}$  M), and  $\mathbf{1}\text{-MeIm}$  ( $5 \times 10^{-5}$  M)

The  $[\text{Fe}^{\text{III}}(\text{TDCPP})\text{Cl}]/\mathbf{1}/\mathbf{1}\text{-MeIm}$  system was irradiated for 30 minutes in the presence of 760 torr of  $\text{O}_2$ . HPLC analyses revealed the formation of both *N*-(4-chlorophenyl)urea (**2**) and *N*-(4-chlorophenyl)cyanamide (**3**; Scheme 3), by comparison of their retention times with those of authentic samples, and by co-injection with the authentic compounds.

Table 2 reports the yields of the described photoprocess in terms of amount of detected products. The first row of this table provides evidence that the urea **2** is the main end-product of the hydroxyguanidine **1**. In agreement with an NOS-like oxidation mechanism, the conversion of **1** to **2** approximately matches the formation of  $\text{NO}$ , which was revealed in the form of its stable end-products  $\text{NO}_2^-$  and  $\text{NO}_3^-$ . Table 2 shows that the cyanamide **3** is a second minor photoproduct. Literature data show that the oxidation of the hydroxyguanidine **1** to the corresponding cyanamide is accompanied by the formation of  $\text{NO}^-$  instead of  $\text{NO}$ .<sup>[14]</sup> This intermediate, after dimerization, protonation and dehydration would release gaseous  $\text{N}_2\text{O}$  without the formation of  $\text{NO}_2^-$  and  $\text{NO}_3^-$ .

Control experiments indicated that the formation of **2**, **3**,  $\text{NO}_2^-$  and  $\text{NO}_3^-$  from **1** did not occur in appreciable amounts in the dark or in the absence of either  $[\text{Fe}^{\text{III}}(\text{TDCPP})\text{Cl}]$  or  $\text{O}_2$ . We also verified that the photoexciting wavelengths employed here did not cause any appreciable degradation of **2** and **3**. Finally, we found UV/Vis evidence that neither **2** nor **3** competes with **1** in binding the metal centre at the concentrations that they typically reach during the photochemical experiment.

$[\text{Fe}^{\text{III}}(\text{TDCPP})\text{Cl}]$  underwent significant spectral changes when irradiated in the presence of **1** and  $\mathbf{1}\text{-MeIm}$ . As shown in Table 1 (compare runs c and e), we observed a blue shift



Scheme 4. Proposed photooxidation mechanism

Table 2. Oxidation of **1** by photoexcited [Fe<sup>III</sup>(TDCPP)Cl] and by the [Fe<sup>III</sup>(TpivPP)(O<sub>2</sub>·)(1-MeIm)] adduct

System	Products <sup>[a]</sup> (μM) Urea <b>2</b>	Cyanamide <b>3</b>	NO <sub>2</sub> <sup>-</sup>	NO <sub>3</sub> <sup>-</sup>
Fe <sup>III</sup> (TDCPP)Cl/1/1-MeIm <sup>[b]</sup>	6.6 ± 0.6	1.5 ± 0.1	2.2 ± 0.2	2.7 ± 0.2
Fe <sup>III</sup> (TDCPP)Cl/1 <sup>[b]</sup>	1.6 ± 0.1	1.5 ± 0.1	<0.6	<0.6
Fe <sup>III</sup> (TDCPP)Cl/1/1-MeIm/PBN <sup>[b]</sup>	3.5 ± 0.3	1.5 ± 0.1	1.2 ± 0.2	1.3 ± 0.2
Fe <sup>III</sup> (TpivPP)(O <sub>2</sub> ·)/1/1-MeIm <sup>[c]</sup>	1 ± 0.1	<0.2	<0.6	<0.6

<sup>[a]</sup> Results are expressed in μmol dm<sup>-3</sup> of products formed and are averages (± standard deviation) of between three and five experiments.

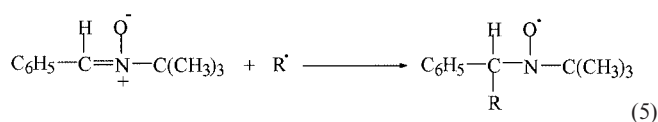
<sup>[b]</sup> Irradiations were carried out at 22 ± 1 °C in the presence of 760 Torr of oxygen. Excitation wavelength: λ > 350 nm. Irradiation time: 30 minutes. [Fe<sup>III</sup>(P)]: 1 × 10<sup>-5</sup> M; [**1**]: 1 × 10<sup>-3</sup> M; [1-MeIm]: 5 × 10<sup>-5</sup> M; [PBN]: 1 × 10<sup>-4</sup> M. <sup>[c]</sup> The [Fe<sup>III</sup>(TpivPP)(O<sub>2</sub>·)]/1-MeIm adduct was obtained by dissolving [Fe<sup>III</sup>(TpivPP)Cl] (1 × 10<sup>-5</sup> M) in a mixture of acetone and ethanol (95:5, v/v) in the presence of 1-MeIm (5 × 10<sup>-5</sup> M). The solution was degassed (less than 1 × 10<sup>-5</sup> Torr), irradiated (90 s) and put in contact with O<sub>2</sub> at low temperature (-5 to -8 °C). Then, **1** (1 × 10<sup>-3</sup> M) was added to the obtained sample.

of the porphyrin Soret band from 426 nm to 416 nm, as well as the formation of two new bands at 505 and 546 nm. These spectral variations may be ascribed to axial coordination of the end-product NO<sub>2</sub><sup>-</sup> anion on the basis of literature data concerning the effect of binding of this anion on the spectroscopic properties of iron porphyrin complexes<sup>[15]</sup> and by the observation that progressive addition of NaNO<sub>2</sub> to the [Fe<sup>III</sup>(TDCPP)]/1/1-MeIm system induced analogous spectral variations.

The data reported in the second line of Table 2 show that the photoinduced oxidation of **1** occurred to some extent also in the absence of 1-MeIm. On the other hand, a significant reduction in the production of **2** and NO was observed in this case, indicating the main role of coordinated 1-MeIm in the photoinduced formation of these products.

### Spin-Trapping Investigation and Proposed Reaction Pathways

Evidence for the oxidation of bound *N*-hydroxyguanidine (**1**) to radical species was provided by an ESR spin-trapping investigation. This technique is a powerful tool for detecting the formation of short-lived radicals<sup>[16]</sup> and has been fruitfully employed in photochemical studies on iron porphyrins.<sup>[2a,4]</sup> It is based on the ability of some molecules, such as α-phenyl-*N*-tert-butyl nitron (PBN), to trap radicals (R<sup>·</sup>) and give paramagnetic nitroxides stable enough to be studied by ESR spectroscopy [Equation (5)].



The [Fe<sup>III</sup>(TDCPP)Cl]/1/1-MeIm system was irradiated in the presence of PBN (5 × 10<sup>-3</sup> M) directly in the cavity of an ESR spectrometer. Figure 3 shows that the spectrum obtained consists of a triplet of doublets, with hyperfine splitting constants *a*<sub>N</sub> = 14.75 G and *a*<sub>H</sub> = 2.77 G. This signal may be ascribed to the trapping of a radical species originating from the photooxidation of the bound hydroxyguanidine **1** according to step b in Scheme 4. In line with

this statement, blank experiments carried out without **1** did not give any ESR signal.

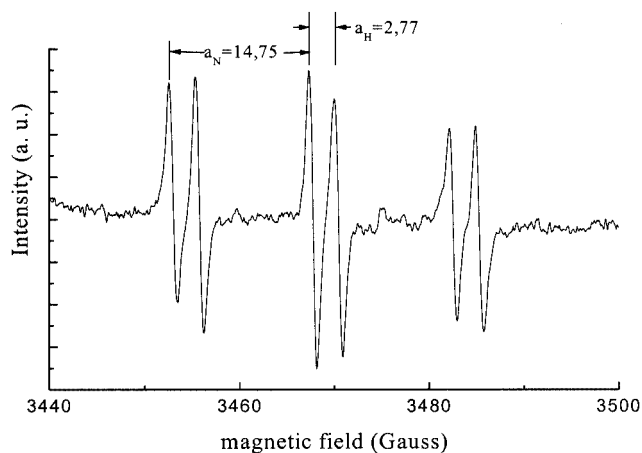


Figure 3. ESR spin-trapping spectrum obtained during irradiation of a CH<sub>3</sub>CN solution of [Fe<sup>III</sup>(TDCPP)Cl] (1 × 10<sup>-5</sup> M) in the presence of **1** (1 × 10<sup>-3</sup> M), 1-MeIm (5 × 10<sup>-5</sup> M) and PBN (5 × 10<sup>-3</sup> M).

Row 3 in Table 2 reports the concentration of **2**, **3**, NO<sub>2</sub><sup>-</sup> and NO<sub>3</sub><sup>-</sup> after 30 minutes irradiation of the [Fe<sup>III</sup>(TDCPP)Cl]/1/1-MeIm system carried out in the presence of PBN (1 × 10<sup>-4</sup> M). The radical scavenger did not affect at all the formation of the cyanamide **3**, while it partially inhibited the production of the urea **2**, NO<sub>2</sub><sup>-</sup> and NO<sub>3</sub><sup>-</sup>.

The above results are consistent with a reaction pathway for the light-induced oxidation of the hydroxyguanidine **1** by [Fe<sup>III</sup>(TDCPP)Cl] that resembles the radical-type autooxidation mechanism mentioned in the introduction.<sup>[5d,10]</sup> In line with the general mechanism shown in Equations (1)–(3), peroxidic intermediates should be formed as a consequence of the very fast reaction of O<sub>2</sub> with the photo-generated ferrous porphyrin in the presence of iminoxyl radicals (steps c and d in Scheme 4). The formation of the urea **2** and NO likely occurs as a consequence of a homolytic cleavage of the O–O bond according to steps e and f. The possibility that photogenerated alkyl hydroperoxides may decompose by the above reactions has been reported previously.<sup>[1c,2]</sup> It seems likely that the well-known ability of



bound 1-MeIm to stabilize this photogenerated ferrous-dioxy intermediate  $\text{Fe}^{\text{II}}(\text{O}_2)^{[12b]}$  may be the reason for the observed positive effect of this nitrogen base on the final product yields.

An additional possibility to take into account is that oxidation of **1** may occur as a consequence of its reaction with  $\text{O}_2^{\cdot-}$ , which could originate from  $\text{Fe}^{\text{III}}(\text{O}_2^{\cdot-})$  dissociation (steps g and h). Indeed, it has been already demonstrated that  $\text{O}_2^{\cdot-}$  can react with **1** to give the cyanamide **3** as the major product.<sup>[17]</sup> The low yield of this product indicates that this possibility is only a minor process in the photoinduced oxidation of **1** described here.

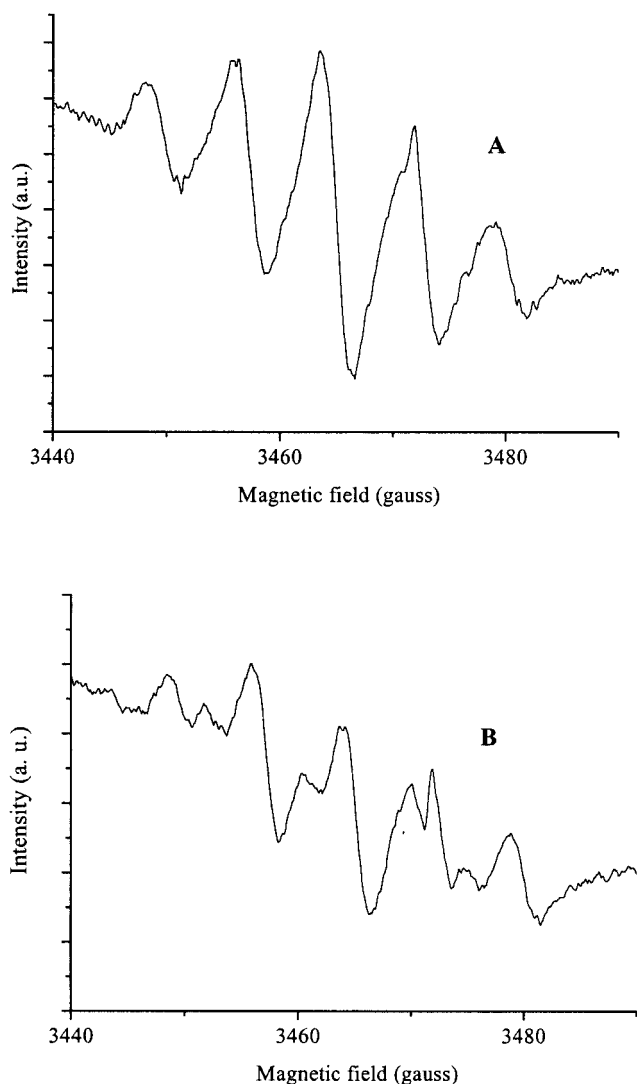
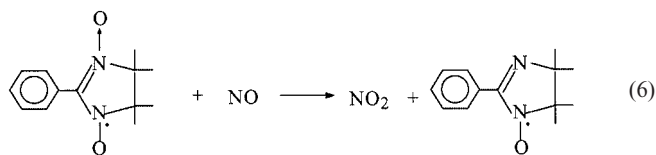


Figure 4. A) ESR spectrum of PTIO ( $2 \times 10^{-6}$  M) in a  $\text{CH}_3\text{CN}$  solution containing **1** ( $1 \times 10^{-3}$  M),  $[\text{Fe}^{\text{III}}(\text{TDCPP})\text{Cl}]$  ( $1 \times 10^{-5}$  M) and 1-MeIm ( $5 \times 10^{-5}$  M); B) curve A after ten minutes irradiation

The ESR spin-trapping technique was also used to obtain direct evidence for the formation of NO. We employed 2-phenyl-4,4,5,5-tetramethylimidazoline-1-oxyl 3-oxide (PTIO) as an NO-specific reactant.<sup>[18]</sup> The ESR spectrum of PTIO consists of a 1:2:3:2:1 quintet due to the interaction of one unpaired electron with two equivalent nitrogen atoms ( $a_{\text{N}} = 8.2$  G). Nitric oxide reacts with this compound according to Equation (6) to give an imino-nitroxide (PTI), in which two different nitrogen atoms generate a different and more complex spectrum with nine lines ( $a_{\text{N}}^1 = 9.8$  G and  $a_{\text{N}}^2 = 4.4$  G).

Curve A in Figure 4 shows the five-line ESR spectrum of PTIO ( $2 \times 10^{-6}$  M) in the presence of **1** ( $1 \times 10^{-3}$  M),  $[\text{Fe}^{\text{III}}(\text{TDCPP})\text{Cl}]$  ( $1 \times 10^{-5}$  M) and 1-MeIm ( $5 \times 10^{-5}$  M). The same signals were obtained when **1** or  $[\text{Fe}^{\text{III}}(\text{TDCPP})\text{Cl}]$  or 1-MeIm were omitted from the reaction mixture. Ten-minute photoexcitation led to a decrease of the intensity of this spectrum together with the growth of new signals, as shown by Curve B in Figure 4. The position of these signals corresponds very well to that expected for the nitroxide PTI.<sup>[17]</sup> Negligible spectral changes were observed in the dark when the photochemical experiment was carried out in the absence of  $[\text{Fe}^{\text{III}}(\text{TDCPP})\text{Cl}]$  or **1**.

#### Reactivity of Photogenerated $[\text{Fe}^{\text{II}}(\text{TpivPP})(\text{O}_2)(1\text{-MeIm})]$

Irradiation of  $[\text{Fe}^{\text{III}}(\text{TpivPP})\text{Cl}]$  in the presence of **1**, 1-MeIm and  $\text{O}_2$  gave results very similar to those obtained with the  $[\text{Fe}^{\text{III}}(\text{TDCPP})\text{Cl}]/1/1\text{-MeIm}$  system from a qualitative point of view. However, experiments carried out with this porphyrin allowed us to accumulate only traces of the end-products, because it undergoes a very fast degradation under aerobic photochemical conditions to give small colourless fragments. This instability may be ascribed to the lack of hindered groups able to protect the *meso* positions from oxidative attacks.

In spite of this limitation, which forced us to limit the photocatalytic characterization previously described to  $[\text{Fe}^{\text{III}}(\text{TDCPP})\text{Cl}]$ , with  $[\text{Fe}^{\text{III}}(\text{TpivPP})\text{Cl}]$  we could obtain direct experimental evidence of the photoinduced formation of a  $[\text{Fe}^{\text{II}}(\text{TpivPP})(\text{O}_2)(1\text{-MeIm})]$  adduct, which, in the previous discussion, has only been supposed for  $[\text{Fe}^{\text{III}}(\text{TDCPP})\text{Cl}]$ .

The first step for obtaining the  $[\text{Fe}^{\text{II}}(\text{TpivPP})(\text{O}_2)(1\text{-MeIm})]$  adduct was the photoinduced reduction of the ferric porphyrin under anaerobic conditions. This result was obtained by irradiating (for 90 s,  $\lambda > 350$  nm) deoxygenated solutions of  $[\text{Fe}^{\text{III}}(\text{TpivPP})\text{Cl}]$  ( $1 \times 10^{-5}$  M) containing 1-MeIm ( $5 \times 10^{-5}$  M). We decided to use an acetone/ethanol (95:5) mixture as solvent knowing that, in these conditions, ethanol works as coordinating solvent and that the primary photochemical process is expected to be the reduction of  $\text{Fe}^{\text{III}}$  to  $\text{Fe}^{\text{II}}$  by the bound ethanolate, in line with the general mechanism shown in Equation (1).<sup>[2,4]</sup> Accordingly, the UV/Vis spectrum observed after irradiation (Curve A in Figure 5) presents the typical absorption at 567 nm of the ferrous porphyrin. The spectral changes (Curve B) that accompany the subsequent oxygenation of the sample at low temperature ( $-5$  to  $-8$  °C) are consistent with the forma-

tion of  $[\text{Fe}^{\text{II}}(\text{TpivPP})(\text{O}_2)(1\text{-MeIm})]$  or  $[\text{Fe}^{\text{III}}(\text{TpivPP})(\text{O}_2\cdot)(1\text{-MeIm})]$  adduct.<sup>[12]</sup>

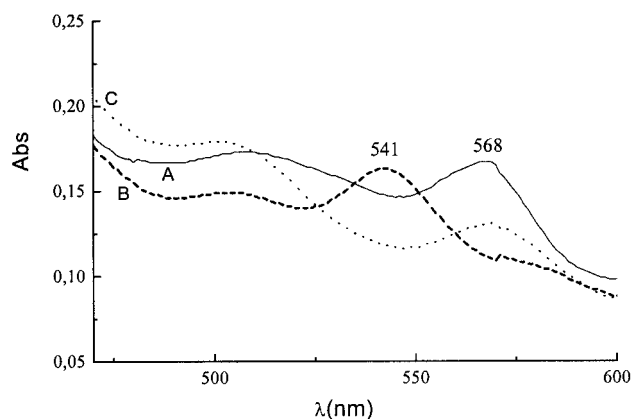
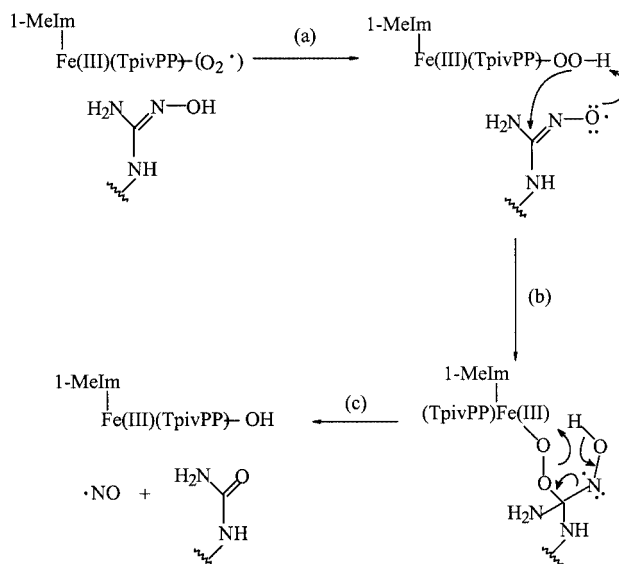


Figure 5. A) UV/Vis spectrum of an acetone/ethanol (95:5) solution of  $[\text{Fe}^{\text{III}}(\text{TpivPP})\text{Cl}]$  ( $1 \times 10^{-5}$  M) and 1-MeIm ( $5 \times 10^{-5}$  M) after 90 s irradiation under anaerobic conditions; B) curve A after subsequent oxygenation of the sample at  $-8^\circ\text{C}$ ; C) curve B after a second deoxygenation

A second deoxygenation of this solution regenerated the spectrum of the ferrous porphyrin deprived of  $\text{O}_2$ . Figure 5 shows that this oxygenation/deoxygenation cycle is not completely reversible, probably due to irreversible oxidation of the porphyrin ring. The  $\text{O}_2$  binding reversibility to  $\text{Fe}^{\text{II}}(\text{TpivPP})$  has been demonstrated and discussed in depth by Collman in previous fundamental papers.<sup>[12]</sup> The novelty of this work is that we observe the same binding reversibility using light rather than chemical reducing agents.

The possibility of accumulating significant amounts of the  $[\text{Fe}^{\text{II}}(\text{TpivPP})(\text{O}_2)(1\text{-MeIm})]$  adduct enabled us to investigate its possible reactivity towards the hydroxyguanidine **1**. In fact, it should be taken into account that the  $[\text{Fe}^{\text{II}}(\text{TpivPP})(\text{O}_2)(1\text{-MeIm})]$  species might undergo reduction by **1** to give an iron-peroxo intermediate,<sup>[19]</sup> although a number of results seem to argue against a reaction between the  $\text{Fe}^{\text{III}}(\text{P})(\text{O}_2\cdot)$  of NOS and *N*-hydroxy-L-arginine.<sup>[9a,9b,20]</sup>

Table 2 shows that the addition of **1** to the photo-generated  $[\text{Fe}^{\text{III}}(\text{TpivPP})(\text{O}_2\cdot)(1\text{-MeIm})]$  led to a detectable amount of urea **2** with a yield of 80% with respect to the sum of **2** and **3**. A possible reaction pathway explaining this result is given in Scheme 5. The  $[\text{Fe}^{\text{III}}(\text{TpivPP})(\text{O}_2\cdot)(1\text{-MeIm})]$  intermediate might abstract the hydrogen atom of the hydroxyguanidine hydroxy group to furnish a hydroperoxo complex (step a), whose well-known nucleophilicity should allow it to react with the iminoxy radical (step b).<sup>[19,21]</sup> Finally, a subsequent pericyclic reaction of the peroxy intermediate is expected to form NO and **2** according to step c. The possibility that the conversion of **1** to **2** and NO upon irradiation of the  $[\text{Fe}^{\text{III}}(\text{TDCPP})\text{Cl}]/1/1\text{-MeIm}$  system may also occur, at least in part, through the described mechanism cannot be ruled out.



Scheme 5. Oxidation of **1** by the  $[\text{Fe}^{\text{III}}(\text{TpivPP})(\text{O}_2\cdot)(1\text{-MeIm})]$  adduct

The formation of urea as a major product of the reaction between  $[\text{Fe}^{\text{II}}(\text{TpivPP})(\text{O}_2)(1\text{-MeIm})]$  and **1** was confirmed by an additional experiment where the  $[\text{Fe}^{\text{II}}(\text{TpivPP})(\text{O}_2)(1\text{-MeIm})]$  adduct was prepared with a chemical reducing agent according to previous work (see Exp. Sect.).<sup>[12b]</sup> Addition of the hydroxyguanidine **1** to the chemically obtained  $[\text{Fe}^{\text{II}}(\text{TpivPP})(\text{O}_2)(1\text{-MeIm})]$  led to the formation of a detectable amount of the urea **2** with a yield of about the 65% with respect to the sum of **2** and **3**. This chemoselectivity in the production of urea is in line with that obtained using light to form  $[\text{Fe}^{\text{II}}(\text{TpivPP})(\text{O}_2)(1\text{-MeIm})]$ . The observed small differences of the **2**:**3** concentration ratios may be ascribed to the experimental error inherent in the HPLC analysis and to the different experimental conditions that we were forced to employ in the two approaches.

## Conclusion

The aforementioned results show that photochemical excitation of iron porphyrins is a suitable means of inducing the oxidation of the hydroxyguanidine **1**. This reaction presents important similarities with the oxidation of the endogenous *N*-hydroxy-L-arginine by heme-containing metalloenzyme nitric oxide synthases (NOSs) and their model systems.

Coordinated hydroxyguanidine **1** presents a photoreactivity that typically characterizes many axial ligands, undergoing oxidation to radical species. The simultaneous formation of  $\text{Fe}^{\text{III}}(\text{O}_2\cdot)$  is a key point for the oxidation of **1**.

The two iron porphyrin complexes employed here have provided complementary results. Photochemical excitation of  $[\text{Fe}^{\text{III}}(\text{TDCPP})\text{Cl}]$  in the presence of  $\text{O}_2$  and 1-MeIm revealed that the urea **2** is the main end-product of **1**. In agreement with an NOS-like oxidation mechanism, the conversion of **1** to **2** approximately matches the formation of

NO, as revealed by both ESR spin-trapping experiments, and in the form of its stable end-products  $\text{NO}_2^-$  and  $\text{NO}_3^-$ . A significant reduction in the production of **2** and NO was observed in the absence of 1-MeIm, due to the main role of coordinated 1-MeIm in stabilizing the  $\text{Fe}^{\text{III}}(\text{O}_2^-)$  intermediate.

The ability of radical scavengers to inhibit the production of both the urea **2** and NO strongly supports the possibility that the reaction pathway resembles a radical-type autoxidation mechanism, where the very fast reaction of  $\text{O}_2$  with the ferrous porphyrin in the presence of the photogenerated iminoxyl radical should yield an iron-peroxo intermediate as precursor of **2** and NO.

The use of  $[\text{Fe}^{\text{III}}(\text{TpivPP})\text{Cl}]$  provides the first experimental evidence for the photoinduced formation of an iron-dioxy adduct. Moreover, the observed reactivity of the  $[\text{Fe}^{\text{II}}(\text{TpivPP})(\text{O}_2)(1\text{-MeIm})]$  complex indicates that iron-peroxo species able to generate the urea **2** may be also formed as a consequence of the reduction of the  $\text{Fe}^{\text{III}}(\text{O}_2^-)$  intermediate by the hydroxyguanidine **1** itself.

The described results give important indications about the reactivity of iron-dioxy complexes that are in good agreement with current opinion on the second step of NOS catalysis. In particular, our results are in line with the hypothesis that the formation of iron-peroxo intermediates is essential for the oxidation of *N*-hydroxy-L-arginine to L-citrulline and NO.

## Experimental Section

**Materials:** The complexes  $[\text{Fe}^{\text{III}}(\text{TDCPP})\text{Cl}]$  and  $[\text{Fe}^{\text{III}}(\text{TpivPP})\text{Cl}]$  were prepared and purified as described elsewhere.<sup>[22,12b]</sup> The hydroxyguanidine **1**, the urea **2** and the cyanamide **3** were synthesized following previous procedures.<sup>[11a]</sup> *N*-Methyl imidazole (1-MeIm),  $\alpha$ -phenyl-*N*-tert-butyl nitron (PBN) and  $\text{NaNO}_2$  were commercial products (Aldrich), 2-phenyl-4,4,5,5-tetramethylimidazoline-1-oxyl 3-oxide (PTIO) was purchased from Alexis Biochemicals. They were all used as received. Acetonitrile, acetone and ethanol were spectroscopic-grade solvents.

**Apparatus:** UV/Vis spectra were recorded with a Kontron Model Uvikon 943 spectrophotometer and X-Band electron spin resonance (ESR) spectra with a Bruker 220 SE spectrometer that was calibrated with  $\alpha,\alpha'$ -diphenylpicrylhydrazyl. HPLC analysis was carried out with a Thermo Quest instrument, equipped with a UV detector, using a Discovery HS PEG column (Supelco, 25 cm  $\times$  4.6 mm, 5  $\mu\text{m}$ ).

Irradiation was carried out with a medium-pressure Hanau Q 400 mercury lamp (15 mW/cm<sup>2</sup>). The required wavelength interval was selected by using cut-off filters. When necessary, solutions were degassed to less than  $1 \times 10^{-5}$  Torr by means of five vacuum-line freeze-pump-thaw cycles. Low temperature experiments were performed in a Julabo F12 (MP) cryostat.

**Photooxidation of *N*-(4-Chlorophenyl)-*N'*-hydroxyguanidine (**1**):**  $[\text{Fe}^{\text{III}}(\text{TDCPP})\text{Cl}]$  or  $[\text{Fe}^{\text{III}}(\text{TpivPP})\text{Cl}]$  ( $1 \times 10^{-5}$  M) was dissolved in a  $\text{CH}_3\text{CN}$  solution (3 mL) containing **1** ( $1 \times 10^{-3}$  M), with or without 1-MeIm ( $5 \times 10^{-5}$  M). When necessary PBN ( $1 \times 10^{-4}$  M) was also added. The solutions thus obtained were irradiated for 30 minutes with wavelengths higher than 350 nm in the presence of

760 Torr of  $\text{O}_2$ . UV/Vis spectra were recorded during the preparation of the solutions after the addition of each component and at the end of the irradiation. HPLC analysis was performed on the irradiated sample. Separation and detection of **1**, **2** and **3** was achieved by eluting with a mixture of  $\text{H}_2\text{O}$  and  $\text{CH}_3\text{CN}$  (85:15) in the presence of  $\text{CH}_3\text{COO NH}_4$  buffer (10 mM), while HPLC analysis of  $\text{NO}_2^-$  and  $\text{NO}_3^-$  was realised using a water solution of acetic acid (pH 3) for elution. In both cases the flow rate was 1 mL/min. Compounds **1**, **2** and **3** were identified by injection of authentic samples. Quantitative analysis was performed using calibration curves obtained from the authentic compounds. Control HPLC experiments were carried out in order to verify that no reaction occurred when irradiation was carried out in the absence of  $[\text{Fe}^{\text{III}}(\text{TDCPP})\text{Cl}]$  or  $\text{O}_2$ . Moreover, we verified that no thermal reaction occurred when the reaction mixture was kept in the dark for several hours.

**ESR Spin-Trapping:**  $\text{CH}_3\text{CN}$  solutions of  $[\text{Fe}^{\text{III}}(\text{TDCPP})\text{Cl}]$  ( $1 \times 10^{-5}$  M) containing **1** ( $1 \times 10^{-3}$  M), 1-MeIm ( $5 \times 10^{-5}$  M) and PBN ( $5 \times 10^{-3}$  M) were irradiated ( $\lambda > 350$  nm, room temperature) inside the ESR cavity using a flat quartz cell. No ESR signal was obtained when performing the described experiment in the absence of **1**.

For NO detection experiments,  $\text{CH}_3\text{CN}$  solutions of  $[\text{Fe}^{\text{III}}(\text{TDCPP})\text{Cl}]$  ( $1 \times 10^{-5}$  M), 1-MeIm ( $5 \times 10^{-5}$  M) and PTIO ( $2 \times 10^{-6}$  M) with and without **1** ( $1 \times 10^{-3}$  M) were irradiated ( $\lambda > 360$  nm) inside the ESR cavity for some minutes.

**Preparation of the  $[\text{Fe}^{\text{II}}(\text{TpivPP})(\text{O}_2)(1\text{-MeIm})]$  Adduct:**  $[\text{Fe}^{\text{III}}(\text{TpivPP})\text{Cl}]$  ( $1 \times 10^{-5}$  M) dissolved in a mixture of acetone and ethanol (95:5, v/v) in the presence of 1-MeIm ( $5 \times 10^{-5}$  M) was degassed to less than  $1 \times 10^{-5}$  Torr by means of five vacuum-line freeze-pump-thaw cycles. Subsequently, it was irradiated (for 90 s) at low temperature ( $-5$  to  $-8$  °C) at wavelengths higher than 350 nm. After irradiation, the solution was put in contact with  $\text{O}_2$  at the same low temperature. Finally, a new deoxygenation cycle was carried out. UV/Vis spectra were recorded after each step of the procedure. HPLC analysis was carried out in order to investigate the reactivity of the hydroxyguanidine **1** ( $1 \times 10^{-3}$  M) with the  $\text{Fe}^{\text{II}}(\text{TpivPP})(\text{O}_2)$  adduct.

The  $\text{Fe}^{\text{II}}(\text{TpivPP})(\text{O}_2)$  adduct was also chemically prepared starting from  $[\text{Fe}^{\text{III}}(\text{TpivPP})(\text{Br})]$  and following the procedure already reported by Collman et al.<sup>[12b]</sup> Here, we employed zinc amalgam as a reducing agent instead of  $[\text{Cr}(\text{acac})_2]_2$ .  $[\text{Fe}^{\text{III}}(\text{TpivPP})(\text{Br})]$  ( $1 \times 10^{-3}$  M) and 1-MeIm ( $3 \times 10^{-3}$  M) dissolved in acetone were degassed by means of three vacuum-line freeze-pump-thaw cycles. A drop of zinc amalgam was then introduced into the solution kept under argon atmosphere. After a while, the solution became red in colour and the appearance of an intense band at 535 nm was indicative of the formation of the  $[\text{Fe}^{\text{II}}(\text{TpivPP})(1\text{-MeIm})_2]$  complex. The solution containing the ferrous complex, separated from the zinc amalgam, in a bath of ethanol/liquid nitrogen at  $-60$  °C was put in contact with  $\text{O}_2$ . Evidence for the formation of the  $[\text{Fe}^{\text{II}}(\text{TpivPP})(\text{O}_2)(1\text{-MeIm})]$  complex was obtained at room temperature by UV/Vis spectroscopy (observation of a new band at 548 nm). Addition of the hydroxyguanidine **1** ( $2 \times 10^{-2}$  M) to an acetone solution of  $[\text{Fe}^{\text{II}}(\text{TpivPP})(\text{O}_2)(1\text{-MeIm})]$  ( $1 \times 10^{-3}$  M) was carried in an ice bath at 0 °C. The reaction mixture was stirred and kept at the same temperature for 30 min before the HPLC analysis.

## Acknowledgments

Financial support from MIUR and CNR is gratefully acknowledged.



- [1] [1a] A. Maldotti, A. Molinari, R. Amadelli, *Chem. Rev.* **2002**, *102*, 3811–3836. [1b] B. Meunier, A. Robert, G. Pratviel, J. Bernadou, in *The Porphyrin Handbook* (Eds.: K. M. Kadish, K. M. Smith, R. Guilard), Academic Press, San Diego, **2000**, vol. 4, 119–174. [1c] A. Maldotti, L. Andreotti, A. Molinari, V. Carassiti, *J. Biol. Inorg. Chem.* **1999**, *4*, 154–161. [1d] L. Weber, R. Hommel, J. Behling, G. Haufe, H. Hennig, *J. Am. Chem. Soc.* **1994**, *116*, 2400–2408. [1e] K. S. Suslick, R. A. Watson, *New J. Chem.* **1992**, *16*, 633–642.
- [2] [2a] A. Maldotti, C. Bartocci, G. Varani, A. Molinari, P. Battioni, D. Mansuy, *Inorg. Chem.* **1996**, *35*, 1126–1131. [2b] A. Maldotti, A. Molinari, L. Andreotti, M. Fogagnolo, R. Amadelli, *Chem. Commun.* **1998**, 507–508. [2c] A. Maldotti, L. Andreotti, A. Molinari, G. Varani, G. Cerichelli, M. Chiarini, *Green Chem.* **2001**, *3*, 42–46. [2d] R. D. Arasasingham, A. L. Balch, C. R. Cornman, L. Latos-Grazynski, *J. Am. Chem. Soc.* **1989**, *111*, 4357–4363. [2e] A. L. Balch, R. L. Hart, L. Latos-Grazynski, T. G. Traylor, *J. Am. Chem. Soc.* **1990**, *112*, 7382–7388.
- [3] R. L. Cheng, L. Latos-Grazynski, A. L. Balch, *Inorg. Chem.* **1982**, *21*, 2412–2418.
- [4] C. Bartocci, A. Maldotti, G. Varani, V. Carassiti, P. Battioni, D. Mansuy, *Inorg. Chem.* **1991**, *30*, 1255–1259.
- [5] W. K. Alderton, C. E. Cooper, R. G. Knowles, *Biochem. J.* **2001**, *357*, 593–615. [5b] B. S. S. Masters, K. McMillan, E. A. Sheta, J. S. Nishimura, L. J. Roman, P. Martasek, *FASEB J.* **1996**, *10*, 552–558. [5c] D. Mansuy, J. P. Renaud, in *Cytochrome P450: Structure, Mechanism, and Biochemistry* (Ed.: P. R. Ortiz de Montellano), Plenum Press, New York and London, **1995**, p. 537–574. [5d] J. T. Groves, C. C. Y. Wang, *Curr. Opin. Chem.* **2000**, *4*, 687–695. [5e] G. M. Rosen, P. Tsai, S. Pou, *Chem. Rev.* **2002**, *102*, 1191–1199.
- [6] [6a] B. R. Crane, A. S. Arvai, D. K. Ghosh, C. Wu, E. D. Getzoff, D. J. Stuehr, J. A. Tainer, *Science* **1998**, *279*, 2121–2126. [6b] C. S. Raman, H. Li, P. Martasek, V. Kral, B. S. S. Masters, T. L. Poulos, *Cell* **1998**, *95*, 939–950.
- [7] [7a] J. T. Groves, Y.-Z. Han in *Cytochrome P450: Structure, Mechanism, and Biochemistry* (Ed.: P. R. Ortiz de Montellano), Plenum Press, New York and London, **1995**, p. 3–48. [7b] M. Sono, M. P. Roach, E. D. Coulter, J. H. Dawson, *Chem. Rev.* **1996**, *96*, 2841–2888. [7c] M. Couture, D. J. Stuehr, D. L. Rousseau, N. Bec, A. C. Gorren, C. Voelker, *J. Biol. Chem.* **2000**, *275*, 3201–3205. [7d] B. Mayer, R. Lange, *J. Biol. Chem.* **1998**, *273*, 13502–13508. [7e] K. M. Ruske, M. M. Spiering, M. A. Marletta, *Biochemistry* **1998**, *37*, 15503–15512.
- [8] [8a] D. J. Stuehr, N. S. Kwon, C. F. Nathan, O. W. Griffith, P. L. Feldman, J. Wiseman, *J. Biol. Chem.* **1991**, *266*, 6259–6263. [8b] P. Klatt, K. Schmidt, G. Uray, B. Mayer, *J. Biol. Chem.* **1993**, *268*, 14781–14787.
- [9] [9a] C. Wei, Z. Wang, A. Meade, J. McDonald, D. Stuehr, *J. Inorg. Biochem.* **2002**, *91*, 618–624. [9b] C.-C. Wei, B. R. Crane, D. J. Stuehr, *Chem. Rev.* **2003**, *103*, 2365–2375. [9c] D. Mathieu, Y. M. Frapart, J. F. Bartoli, J. L. Boucher, P. Battioni, D. Mansuy, *Chem. Commun.* **2004**, 54–55.
- [10] C. C. Y. Wang, D. M. Ho, J. T. Groves, *J. Am. Chem. Soc.* **1999**, *121*, 12094–12103.
- [11] [11a] A. Renodon-Corniere, J.-L. Boucher, S. Dijol, D. J. Stuehr, D. Mansuy, *Biochemistry* **1999**, *38*, 4663–4668. [11b] A. Renodon-Corniere, S. Dijol, C. Perollier, D. Lefèvre-Groboillot, J.-L. Boucher, R. Attias, M.-A. Sari, D. J. Stuehr, D. Mansuy, *J. Med. Chem.* **2002**, *45*, 944–954.
- [12] [12a] J. P. Collman, R. R. Gagne, T. R. Halbert, J. C. Marchon, C. A. Reed, *J. Am. Chem. Soc.* **1973**, *95*, 7668–7870. [12b] J. P. Collman, R. R. Gagne, C. A. Reed, T. R. Halbert, G. Lang, W. T. Robinson, *J. Am. Chem. Soc.* **1975**, *97*, 1427–1439.
- [13] [13a] D. Lefèvre-Groboillot, S. Dijols, J. L. Boucher, J. P. Mahy, R. Ricoux, A. Desbois, J. L. Zimmermann, D. Mansuy, *Biochemistry* **2001**, *40*, 9909–9917. [13b] D. Lefèvre-Groboillot, Y. Frapart, A. Desbois, J. L. Zimmermann, J. L. Boucher, A. C. F. Gorren, B. Mayer, D. J. Stuehr, D. Mansuy, *Biochemistry* **2003**, *42*, 3858–3867.
- [14] [14a] M. J. Clague, J. S. Wishnok, M. A. Marletta, *Biochemistry* **1997**, *36*, 14465–14473. [14b] J. Fukuto, G. C. Wallace, R. Hsieh, G. Chaudhuri, *Biochem. Pharmacol.* **1992**, *43*, 607–613.
- [15] Z. Wei, M. D. Ryan, *Inorg. Chim. Acta* **2001**, *314*, 49–53.
- [16] E. G. Janzen, *Acc. Chem. Res.* **1971**, *4*, 31–39.
- [17] [17a] T. Akaike, M. Yoshida, Y. Miyamoto, K. Sato, M. Kohno, K. Sasamoto, K. Miyazaki, S. Ueda, H. Maeda, *Biochemistry* **1993**, *32*, 827–832. [17b] R. Ricoux, J.-L. Boucher, D. Mandon, Y.-M. Frapart, Y. Henry, D. Mansuy, J.-P. Mahy, *Eur. J. Biochem.* **2003**, *270*, 47–55.
- [18] N. Sennequier, J. L. Boucher, P. Battioni, D. Mansuy, *Tetrahedron Lett.* **1995**, *36*, 6059–6062.
- [19] [19a] M. A. Marletta, *J. Biol. Chem.* **1993**, *268*, 12231–12234. [19b] H. G. Korth, R. Sustmann, C. Thater, A. R. Butler, K. U. Ingold, *J. Biol. Chem.* **1994**, *269*, 17776–17779. [19c] H. Huang, J. M. Hah, R. B. Silverman, *J. Am. Chem. Soc.* **2001**, *123*, 2674–2676. [19d] A. R. Hurshman, C. Krebs, D. E. Edmondson, B. M. Huynh, M. A. Marletta, *Biochemistry* **1999**, *38*, 15689–15696.
- [20] Z.-Q. Wang, C. Wei, S. Ghosh, A. L. Meade, C. Hemann, R. Hille, D. J. Stuehr, *Biochemistry* **2001**, *40*, 12819–12825.
- [21] D. L. Wertz, J. S. Valentine, in *Structure and Bonding: Metal-oxo and Metal-peroxo Species in Catalytic Oxidations* (Ed.: B. Meunier), Springer-Verlag, Berlin, Heidelberg, New York, **2000**, *97*, 37–60.
- [22] P. Battioni, J. P. Renaud, J. F. Bartoli, J. F. Reina-Artiles, M. Fort, D. Mansuy, *J. Am. Chem. Soc.* **1988**, *110*, 8462–8470.

Received January 21, 2004

Early View Article

Published Online May 27, 2004